Adsorption and Degradation of 2-Chlorophenol by TiO_2/AC and TiO_2/CB in Photocatalytic Process

Jirapat Ananpattarachai, Puangrat Kajitvichyanukul*

Center of Excellence on Environmental Research and Innovation, Faculty of Engineering, Naresuan University, Phitsanulok 65000, Thailand
puangratk@nu.ac.th

In this work, carbonaceous materials including activated carbon (AC) and carbon black (CB) were used in an enhancement the adsorption capacity of TiO_2 particles. The carbon supported TiO_2 composite materials denoted as TiO_2/AC and TiO_2/CB were prepared by sol–gel method and used in photocatalytic process of 2-chlorophenol in aqueous solution. Results reveal that both AC and CB can increase adsorption capacity of TiO_2 while AC provided highest adsorption of 2-chlorophenol on its surface. Adsorption isotherms for both materials were well explained by Freundlich equation representing a multilayer of 2-chlorophenol adsorbed on titanium dioxide surface. During the irradiation, TiO_2/CB exerted highest removal efficiency and initial reaction rate in 2-chlorophenol degradation among three types of catalysts, TiO_2/CB, TiO_2/AC and TiO_2. The mineralization of 2-chlorophenol was achieved within 200 min for both TiO_2/AC and TiO_2/CB catalysts.

1. Introduction

Recently, modification of immobilized TiO_2 with supported materials has been widely investigated (Laoufi et al., 2013). Among several types of supported materials, activated carbon (AC) has been received highest attention and is widely used (Iovino et al., 2013). The AC was reported as an alternative low-cost adsorbent for removal of dyes (Brahim et al., 2014) and Cr(VI) (Silgado et al., 2014). Owing to its large surface area to adsorb much large quantity of organic substances, it can increase the removal rate of pollutant for TiO_2 photocatalysis process. Two different AC and TiO_2 configurations for pollutant removal have been investigated (Rioja et al., 2014). The first configuration is an aqueous suspension mixture (or slurry) of both components. The mass transfer limitation is a major challenge, and it can be minimized by the well dispersion of TiO_2 powder in suspension. However, in the slurry system, the recovery of TiO_2 particles from discharge effluent is a critical issue due to their small size (Rioja et al., 2014). Another configuration is a composite TiO_2/AC material. TiO_2 nanoparticles were attached to larger particles of AC. This method is found that it can improve process efficiency (Lim et al., 2011) and it can overcome the difficulty in the separation of the catalyst from the treated water. However, owing to the pores (micropores) in the AC is very small, and the diffusion rate of the pollutant adsorbed in the micropores toward the surface of TiO_2 is slow, the enhancement in photodegradation is not as high as expected (Mao and Weng, 2009). To overcome this challenge, the carbon black (CB) has been selected to be a supported material for TiO_2. The fine surface structure and a high electrical conductivity property of CB may lead to a higher photocatalytic efficiency than that of AC.

In this work, adsorption behaviour and reaction kinetics of TiO_2/AC and TiO_2/CB composite materials were investigated. Both AC and CB were used in the enhancement the adsorption capacity of TiO_2 particles. The composite materials both TiO_2/AC and TiO_2/CB were used in photocatalytic process of organic pollutant in aqueous solution. In this work, we selected 2-chlorophenol (2-CP) as a model organic pollutant due to its applications in many industries and its contamination in natural water. The adsorption behaviour of TiO_2/AC and TiO_2/CB on 2-chlorophenol removal was investigated. The reaction kinetics from both catalysts in 2-CP removal has been compared and reported.

2. Materials and methods

2.1 TiO$_2$/AC and TiO$_2$/CB preparation

Sol–gel method was employed to deposit TiO$_2$ onto the surface of AC and CB. AC used in this work was form Sigma–Aldrich (untreated granular, 20-60 mesh). CB used in this work was Vulcan XC-72R (Cabot), which had a BET surface area of 243 m^2·g^{-1}. Titanium (IV)-isopropoxide, (Ti(Opr^i)$_4$, TTIP, 97%) purchased from Alpha Aesar was used as titanium source for the preparation of TiO$_2$ photocatalysts. Titanium precursor was first dissolved in ethanol solution and dispersed with the addition of a proper amount of acetic acids (Sigma-Aldrich, 99.5 %, monohydrate). A homogeneous solution was obtained after 1 h mixed of all reagents. Then, AC or CB was washed with 6N HNO$_3$ and loaded into the solution with the ratios of TiO$_2$ to AC or CB as of 1:10 and mixed for 10 h. Then the mixed solutions were dried at 80 °C overnight and calcined at 400 °C for 1 h to obtain TiO$_2$/AC or TiO$_2$/CB composite catalysts. The Brunauer-Emmett-Teller (BET) surface areas of the samples were measured with N$_2$ adsorption at liquid nitrogen temperature determined by a Quantachrome Autosorb Automated Gas Sorption System. Each sample (~0.06 g) was degassed in 80-150 h at 250 $^{\circ}$C before N$_2$ adsorption. The specific surface area and pore size distribution of the materials were obtained by using the BET analysis.

2.2 Adsorption and Photocatalytic Experiments

Dark adsorption, photolysis, and photocatalytic experiments were performed under the same experimental conditions, by means of kinetic studies from batch experiments at room temperature. Briefly, for adsorption in dark conditions about 1 g·L^{-1} of adsorbent was placed in dark glass flasks containing 400 mL of 2-CP solution (in distilled non-buffered water) of the initial concentration from 1 to 100 mg·L^{-1} (solution pH ca. 6 units). The suspensions were stirred (100 rpm), and small aliquots of the solution (1.5 mL) were taken out at fixed time intervals to measure the evolution of the adsorbate concentration, using a UV spectrometer (Thermo Scientific GENESYS 10S UV-Vis). The extracted samples were reintroduced in the flasks in order to avoid changes in the total volume of solution. Experiments were carried out in a quartz photoreactor of 400 mL aqueous solution. The UV irradiation source was provided by high pressure mercury lamp (125 W from ACE glass), vertically suspended in a cylindrical, double-walled quartz jacket cooled by flowing water, immersed in the solution. The water cell was used to control the temperature during the experiments, preventing any overheating of the suspension due to the irradiation. At regular intervals, aliquots of the solution were extracted and analyzed by GC (Spherisorb C18, 125 mm, 4 mm), using the methanol–water mixtures as a mobile phase, and a photodiode array detector. The samples were previously filtered using regenerated cellulose filter of the mean pore size 0.45 mm.

3. Results and discussion

3.1 Chemical characterization of materials

Activated carbon (AC) and carbon black (CB) were used as catalyst supports for TiO$_2$ (10 wt.%) in the photodegradation of 2-CP. Table 1 shows the BET surface areas and pore size distributions of all employed materials. The specific surface areas of AC, CB, TiO$_2$, TiO$_2$/AC and TiO2/CB were 630, 243, 201, 410.7 and 184.7 m^2·g^{-1}, respectively. It was observed that BET surface areas of carbonaceous materials containing catalyst were smaller than that of original materials (AC and CB) and greater than those of neat TiO$_2$ catalysts. Although AC had a large surface area to adsorb a large quantity of pollutant, the pores (micropores) in the AC were very small (3.4 nm). When TiO$_2$ was loaded on AC surface, the average pore size and the total pore volume of TiO$_2$/AC was smaller than AC. This result is in good agreement with data reported previously (Velasco et al., 2010) that the TiO$_2$ deposited in AC can reduce the surface area and pore volume of AC. The deposition of TiO$_2$ in the activated carbon may partially block the porosity of the support material though the TiO2/AC still had a relatively large pore volume and surface area. Morphologies of TiO$_2$/AC and TiO$_2$/CB have shown in Figure 1.

Table 1: Physico-chemical characteristics of materials

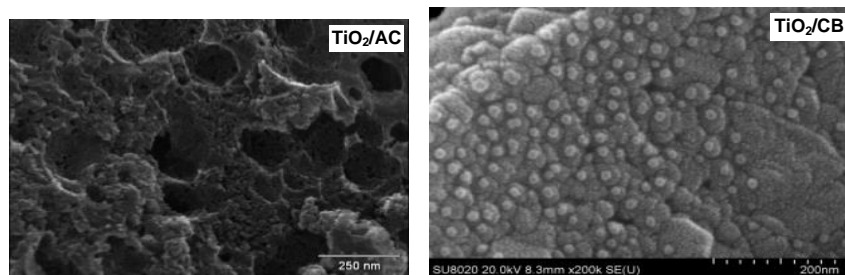| Materials	Surface area (m^2·g^{-1})	Average crystal size (nm)	Average micropore size (nm)	Total pore volume (cm^3·g^{-1})
TiO$_2$	201	10	3.2	0.42
AC	630	-	3.4	0.81
CB	243	30	3.3	0.632
TiO$_2$/AC	410.7	-	3.1	0.535
TiO$_2$/CB	184.7	-	3.1	0.545

Figure 1: Morphologies of TiO$_2$/AC and TiO$_2$/CB

For Table 1, the mean particle size of CB (30 nm) was larger than that of TiO$_2$ (10 nm). With the deposition of TiO$_2$ on the CB surface, the average pore size of TiO$_2$/CB was smaller than that of CB. Mao and Wang (2009) reported that when a small amount of TiO$_2$ was incorporated with CB, the size and the number of pores and the surface area of CB would be reduced. However, when a large number of TiO$_2$ was incorporated with CB, the pore size distribution of TiO$_2$/CB would be dominated by the segregated phase of TiO$_2$ that do not deposit on the exterior and interior surface of CB (Mao and Weng, 2009).

3.2 Adsorption behavior of TiO$_2$/AC and TiO$_2$/CB

The adsorption behaviors of AC, CB, TiO$_2$, TiO$_2$/AC and TiO$_2$/CB in 2-CP removal, in the dark, were investigated. Solution pH were around 6 units in all the experiments; under these conditions 2-CP molecule was mainly in a non-dissociated state (pK$_a$ 8.48), for which interactions between the 2-CP molecule and the adsorbate were predominantly dispersive (non-electrostatic). The initial concentration of 2-CP was 100 mg·L^{-1}. Changes of 2-CP during the adsorption process using CB, AC, TiO$_2$, TiO$_2$/AC, and TiO$_2$/CB are shown in Figure 2.
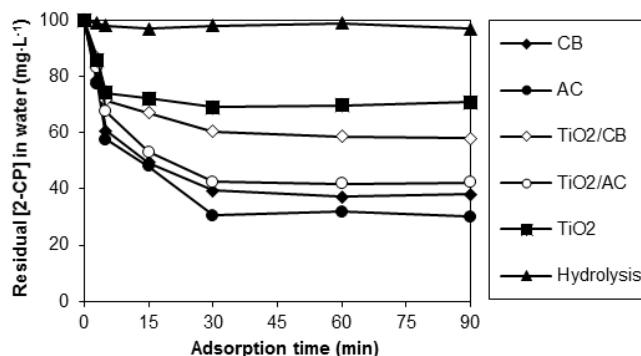

Figure 2: Change of 2-CP in the adsorption process using CB, AC, TiO$_2$, TiO$_2$/AC, and TiO$_2$/CB

Without carbonaceous materials or catalyst in the solution, less amount of 2-CP was degraded by hydrolysis process. The 2-CP removal efficiency by adsorption process using TiO$_2$ bare catalyst was only about 25 % while the 2-CP removal was best removed by activated carbon (removal efficiency 70 %) owing to the highest surface area of this material. The 2-CP removal efficiency of TiO$_2$ was enhanced with the deposition of AC or CB. The maximum adsorption capacity and removal efficiency of the catalyst were tremendous improved as shown in Figure 3 and 4.

3.3 Determination of Adsorption isotherm for TiO$_2$/AC and TiO$_2$/CB

The values of 2-CP adsorption at the equilibrium were used in determining the adsorption isotherm in both Langmuir and Freundlich equations:

$$\frac{C_e}{(x/m)} = \frac{1}{K_L Q} + \frac{C_e}{Q} \tag{1}$$

$$x/m = K_f C_e^{\frac{1}{n}} \tag{2}$$

where C_e is the equilibrium concentration of 2-CP, mg·L^{-1}, x/m is the amount of adsorbed 2-CP at equilibrium per unit mass of TiO$_2$, mg·g^{-1}, and Q and K_L are Langmuir constants related to adsorptive capacity and energy of adsorption, respectively. For Equation 2, K_f is the adsorption capacity and n is the adsorption intensity for Freundlich isotherm. Figure 5 and 6 expresses plots of Freundlich and Langmuir equations for both TiO$_2$/AC and

TiO_2/CB composites according to above equations. The correlation coefficients (R^2) for the linear regression fit of the Freundlich plots for both TiO_2/AC ($R^2 = 0.9917$) and TiO_2/CB ($R^2 = 0.9918$) are higher than that of the Langmuir Plots (0.8355 and 0.7443 for TiO_2/AC and TiO_2/CB, consequently). This information indicated that adsorption isotherms for both TiO_2/AC and TiO_2/CB were well explained by Freundlich equations.
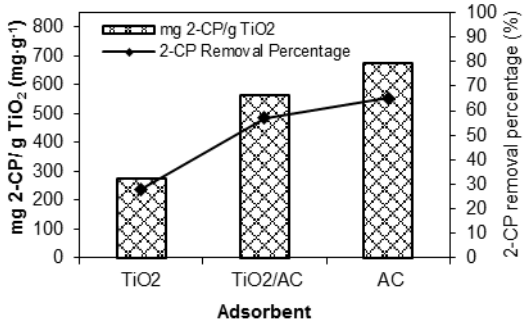

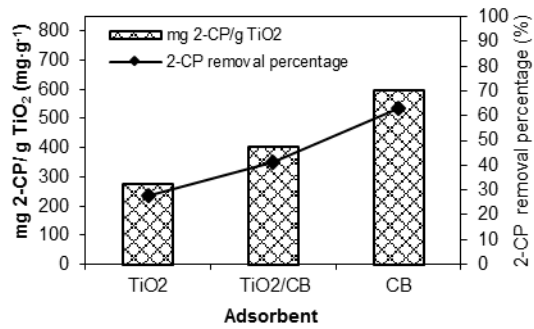Figure 3: Maximum adsorption capacity and removal efficiency of 2-CP by TiO_2, TiO_2/AC, AC

Figure 4: Maximum adsorption capacity and removal efficiency of 2-CP by TiO_2, TiO_2/CB, CB
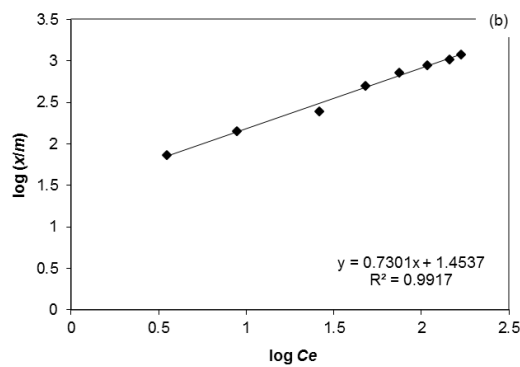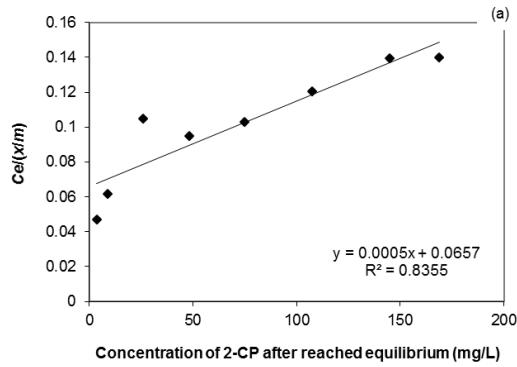

Figure 5: Adsorption isotherm for TiO_2/AC: a) Langmuir isotherm and b) Freundlich isotherm
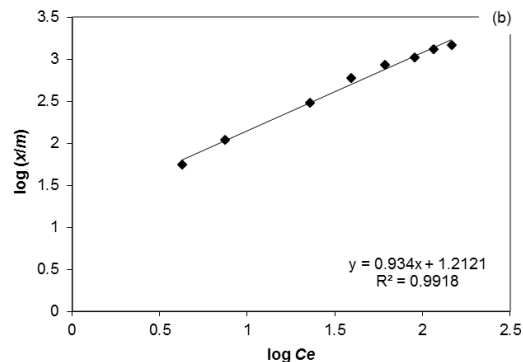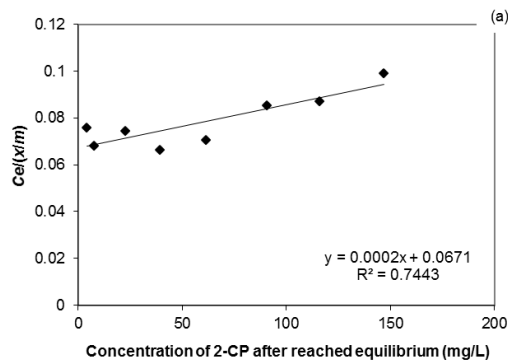

Figure 6: Adsorption isotherm for TiO_2/CB: a) Langmuir isotherm and b) Freundlich isotherm

The adsorption capacity (K_f) and adsorption intensity ($1/n$) of TiO_2/AC was a significant increase from those of TiO_2 and approached those of AC. The K_f values were 9.52, 28.42 and 94.42 $(mmol/kg)^{1-1/n}$ for TiO_2, TiO_2/AC, and AC, respectively. The $1/n$ values were 0.90, 0.73, and 0.58 for TiO_2, TiO_2/AC, and AC, respectively. For TiO_2/CB, using CB as catalyst support also enhanced the adsorption capacity and adsorption intensity of TiO_2 in the same manner with AC. The K_f constants were 9.52, 16.29, and 71.32 $(mmol/kg)^{1-1/n}$ and $1/n$ constants were 0.90, 0.93, and 0.63 for TiO_2, TiO_2/CB, and CB, respectively. In comparison of K_f and n constants, with a higher surface area and total pore volume, AC can enhance the adsorption of 2-CP on the catalyst surface much better than CB as represents by adsorption capacity and adsorption intensity of both TiO_2/AC and TiO_2/CB.

3.4 Photocatalytic Degradation of 2-CP using TiO$_2$/AC and TiO$_2$/CB

Results in Figure 7 show that both AC and CB had no photocatalytic activity under irradiation but can adsorb 2-CP as shown earlier. Both AC and CB can enhance the 2-CP degradation and the removal rates of TiO$_2$/AC and TiO$_2$/CB were much higher than bare TiO$_2$. The increase in the removal rate upon photocatalytic process can be ascribed to the preferential adsorption and surface concentration of the 2-CP onto the carbonaceous material porosity. Consequently, the more rapidly decompose of 2-CP occurred by a spontaneous transfer from the carbonaceous support to the TiO$_2$ surface due to the large concentration gradient between the two solid phases. Results of high photoactivity of carbonaceous supported catalyst found in both TiO$_2$/AC and TiO$_2$/CB in this work is in good agreement with previous works (Lee et al., 2004). The combination of the adsorption capacity of carbon and the photoactivity of titanium oxide (Mao and Weng, 2009) is tentatively the explanation of the enhancement of 2-CP removal
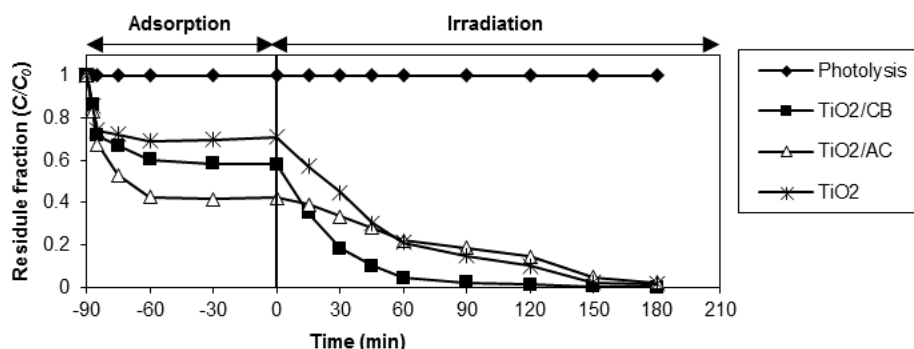

Figure 7: Change of residual fraction of 2-CP during adsorption and irradiation time in photocatalytic process using AC, CB, TiO$_2$, TiO$_2$/AC, and TiO$_2$/CB

Figure 8 shows the change of 2-CP during the irradiation process using TiO$_2$, TiO$_2$/AC, and TiO$_2$/CB. To obtain the intrinsic photocatalytic degradation of these catalysts during irradiation, the amount of 2-CP adsorbed by carbonaceous materials was deducted from the total amount of removed 2-CP. All three catalysts (TiO$_2$, TiO$_2$/AC, and TiO$_2$/CB) can remove 2-CP within 200 min but within different reaction rate. The initial reaction rate in 2-CP degradation are 0.0480, 0.1245, and 0.2547 mg·L^{-1}·min^{-1} for TiO$_2$/AC, TiO$_2$, and TiO$_2$/CB, respectively. The TiO$_2$/CB exhibited the highest reaction rate. The half-life of 2-CP degradation could be arrayed as follow: TiO$_2$/AC< TiO$_2$< TiO$_2$/CB. The difference in reaction rate in 2-CP degradation using TiO$_2$, TiO$_2$/AC, and TiO$_2$/CB could be explained by the action of TiO$_2$ on AC and CB surface. The overall removal rates of all supported catalyst were higher than that of bare TiO$_2$ as shown in Figure 8. However, when the amount of 2-CP adsorbed by carbonaceous materials was deducted from the total amount of removed 2-CP, the intrinsic reaction rate and rate constant of TiO$_2$/CB were higher than that of bare TiO$_2$. On the contrary, the intrinsic reaction rate and rate constant of TiO$_2$/AC were lower than that of bare TiO$_2$.
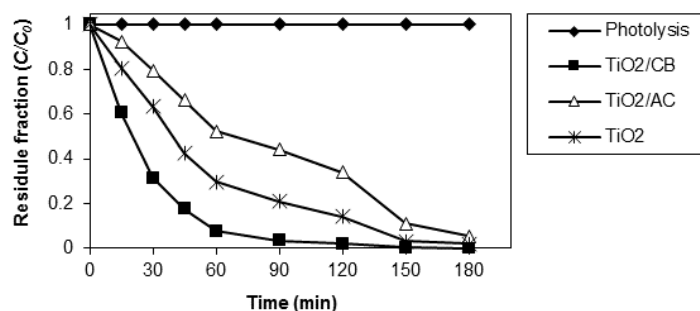

Figure 8: Change of residual fraction of 2-CP during irradiation time only in photocatalytic process using TiO$_2$, TiO$_2$/AC, and TiO$_2$/CB

This information suggests different behavior of TiO$_2$ deposited on AC and CB surface. In the case of AC surface, the greater surface area (630 m^2/g) and, in turn, the higher adsorption capacity of AC was a major factor for 2-CP removal by TiO$_2$/AC composite catalysts. As reported by many previous works (Lee et al., 2004), with a large total pore volume (7.1 cm^3/g), part of the TiO$_2$ precursor deposited in all three parts of the pore network (macropores, mesopores, and micropores) of AC leading topless amount of TiO$_2$ on the exterior surface of AC.

Consequently, AC sheltered the illumination. In addition, the 2-CP adsorbed in micropores of AC cannot easily transfer to the surface of TiO_2. Consequently, low efficiency in intrinsic degradation of 2-CP upon irradiation using TiO_2/AC was seen in Figure 8. For CB consideration, from Table 1, the mean particle size of CB (30 nm) was larger than that of TiO_2 (10 nm). With the equivalent pore size of CB (3.3 nm) compared with that of TiO_2 (3.2 nm); the pore size distribution of TiO_2 and CB were somewhat similar. Moreover, the CB had bigger pores and larger surface than TiO_2. So, CB played a major role as a catalyst support for TiO_2 in enhancing 2-CP adsorption and irradiation. In comparison, CB had fewer micropores than AC and hence less TiO_2 was deposited into the micropores. When TiO_2/CB was applied, the illumination shelter did not tentatively occur causing higher in reaction rate of 2-CP removal than that of 2-CP removal when TiO_2/AC was applied. So, the different performance of carbonaceous supported-TiO_2 caused the difference in pollutant removal efficiency as shown in this work.

4. Conclusion

This paper addressed the comparison of photodegradation enhancement in degradation of organic pollutants using different carbonaceous materials (AC or CB) in photocatalytic process. These enhancements can be achieved by deposition of TiO_2 on the surface of carbonaceous materials (AC and CB). Both AC and CB can increase adsorption capacity of TiO_2. AC enhanced the adsorption capacity on TiO_2/AC and provided the highest adsorption of 2-chlorophenol on its surface. The adsorption capacity constant (K_f) were 28.42 and 16.29 $(mmol/kg)^{1-1/n}$ for TiO_2/AC and TiO_2/CB, respectively. During the irradiation, TiO_2/CB enhanced the photoactivity in 2-CP degradation and exerted the highest performance and highest initial reaction rate in 2-CP degradation when compared with TiO_2/AC and bare TiO_2. The initial reaction rates in 2-CP degradation are 0.0480, 0.1245, and 0.2547 $mg \cdot L^{-1} \cdot min^{-1}$ for TiO_2/AC, TiO_2, and TiO_2/CB, respectively. With large total pore volume of AC, part of the TiO_2 precursor deposited in the micropores of AC leading to less amount of TiO_2 on the exterior surface of AC. Consequently, AC sheltered the illumination. While CB had fewer micropores than AC, less TiO_2 was deposited into the micropores. The illumination shelter did not occur in CB causing higher efficiency in 2-CP removal during the irradiation process. Consequently, the difference in pollutant removal efficiencies of carbonaceous supported catalyst tentatively resulted from the different properties in pore size and total pore volume of both carbonaceous supported materials. This finding showed that both AC and CB in form of TiO_2/AC and TiO_2/CB composite materials could be used effectively in enhancing the photodegradation of organic pollutants.

References

Brahim I.O., Belmedani M., Belgacem A., Hadou H., Sadaoui Z., 2014, Discorloration of azo dye solutions by adsorption on activated carbon prepared from the cryogenic grinding of used tired, Chemical Engineering Transactions, 38,121-126.

Iovino P., Canzano S., Capasso S., Di Natale M., Erto A., Lama A., Musmarra D., 2013, Single and competitive adsorption of toluene and naphthalene onto activated carbon, Chem. Eng. Trans. 32, 67-72.

Laoufi N.A., Hout S., Tassalit D., Ounnar A., Djouadi A., Chekir N., Bentahar F., 2014, Removal of a persistent pharmaceutical micropollutant by UV/TiO_2 process using an immobilized titanium dioxide catalyst: parametric study, Chemical Engineering Transactions, 32, 1951-1956.

Lee D.K., Kim S.C., Kim S.J., Chung I.S., Kim S.W., 2004, Photocatalytic oxidation of microcystin-LR with TiO_2-coated activated carbon, Chem. Eng. J. 102, 93-98.

Lim T., Yap P., Srinivasan M., Fane A.G., 2011, TiO_2/AC composites for synergistic adsorption-photocatalysis processes: present challenges and further developments for water treatment and reclamation. Crit. Rev. Environ. Sci. Technol. 41, 1173-1230.

Mao C.C., Weng H.S., 2009, Promoting effect of adding carbon black to TiO_2 for aqueous photocatalytic degradation of methyl orange, Chem. Eng. J. 155, 744-749.

Rioja N., Benguria P., Peñas F.J., Zorita S., 2014, Competitive removal of pharmaceuticals from environmental waters by adsorption and photocatalytic degradation, Environ. Sci. Pollut. Res. 1, 1-10.

Silgado K.J., Marrugo G.D., Puello J., 2014 Adsorption of chromium (VI) by activated carbon produced from oil palm Endocarp, Chemical Engineering Transactions, 37, 721-726.

Velasco L.F., Parra,J.B., Ania C.O., 2010, Role of activated carbon features on the photocatalytic degradation of phenol, Appl. Surf. Sci. 256, 5254-5258.